Journal of Industrial Microbiology & Biotechnology (1998) 21, 275–282

http://www.stockton-press.co.uk/jim

Generation of a histidine-tagged antibotulinum toxin antibody fragment in *E. coli*: effects of post-induction temperature on yield and IMAC binding-affinity

WE Bentley[1,2], RD Madurawe[1], RT Gill[2], M Shiloach[2], TE Chase[1], TR Pulliam-Holoman[2] and JJ Valdes[3]

[1]*Bioprocess Scale-Up Facility, Engineering Research Center, University of Maryland, College Park, MD 20742;* [2]*Department of Chemical Engineering and Center for Agricultural Biotechnology, University of Maryland, College Park, MD 20742;* [3]*US Army Edgewood Research, Development and Engineering Center (ERDEC), Aberdeen Proving Grounds, MD 21010–5423, USA*

Recombinant *E. coli* clones expressing a 50-kDa poly-histidine tail tagged antibody fragment against botulinum toxin (bt-Fab) were initially screened for yield and binding affinity. One clone was selected for bioprocess development. The selected bt-Fab vector was induced by addition of IPTG and the protein was targeted to the periplasm by inclusion of a *pelB* leader sequence. A histidine$_6$ affinity ligand at the heavy chain C-terminus facilitated single-step purification by immobilized metal-affinity chromatography (IMAC). Notably, the effects of post-induction temperature on bt-Fab expression and downstream purification were evaluated. Our results demonstrated that fermentation conditions interfered with purification on the IMAC column at 37°C. Protease analysis by gelatin polyacrylamide gel electrophoresis (GPAGE) indicated the presence of a membrane-bound ~39 kDa protease activity shortly after induction. The appearance of the protease activity was inversely correlated with the bt-Fab yield. The protease was purified and was shown to degrade bt-Fab. A simple kinetic model was developed describing temporal regulation of protease and bt-Fab degradation. Partially degraded bt-Fab was unrecoverable by IMAC, presumably due to the loss of the His$_6$ affinity ligand. The amount of purified bt-Fab obtained per liter of fermentation broth was typically ~1 mg.

Keywords: Fab antibody expression; *E. coli* fermentation; immobilized metal affinity chromatography (IMAC); proteases; botulinum toxin; temperature sensitivity

Introduction

Antibodies are widely used in many applications such as affinity purification, immunodiagnostics and immunotherapeutics. The high costs associated with antibody production by conventional hybridoma technology or by mammalian cell culture remain a major drawback in their usage, particularly in applications such as immunopurifications where large quantities of antibody are required. Although the expression of antibodies in *E. coli* offers a low-cost alternative, the lack of post-translational modification and its potential impact on protein folding and bioactivity are inherent disadvantages of eukaryotic protein expression in this and other bacterial systems. However, recombinant immunoglobulin libraries produced in bacteria offer a major advantage over hybridoma fusions in that one can generate a large number of clones with a range of epitopic specificities while single fusions give limited epitopic specificities despite extensive immunizations and adequate immune responses. Therefore, by controlled selection of antibody specificity, recombinant immunoglobulin libraries in bacteria can be advantageously used to isolate rare clones with desired specificities that may not be possible with hybridoma fusions. Moreover, the generation of immunoglobulin libraries and subsequent production of the desired clones takes little time relative to hybridoma technology.

Using a combinatorial phage display library, Emanuel *et al* [3] produced a recombinant *E. coli* library expressing a 50-kDa Fab antibody fragment against botulinum neurotoxin serotype B (bt-Fab), a potent neurotoxin produced by the bacterium *Clostridium botulinum*. Initial screening of the combinatorial library yielded clones that were able to recognize non-neurotoxin proteins of the toxin complex in a manner similar to monoclonal antibodies produced by conventional hybridoma fusions. By altering the biopanning selection process, clones encoding antibodies that specifically recognized the neurotoxin component of the botulinum toxin complex were isolated from the combinatorial library. The bt-Fab gene insert was excised from positive clones and inserted into a pHist vector, which is a pSurfscript phagemid, modified to contain a linker encoding six histidines at the C-terminus of the heavy chain. The addition of a histidine tail facilitates recombinant protein purification by immobilized metal affinity chromatography (IMAC). The plasmid vector also contained the *pelB* leader sequence for translocating the bt-Fab to the *E. coli* periplasmic space, thus enabling proper folding and disulfide bond formation. These clones were then screened for expression yield and because the bt-Fab contained the histidine affinity tag, they were rescreened for neurotoxin binding affinity.

Potential problems with the selection of the *pelB* secretory mechanism are the blockage of nascent protein at the inner membrane and proteolytic degradation of both the

Correspondence: Dr WE Bentley, Department of Chemical Engineering and Center for Agricultural Biotechnology, University of Maryland, College Park, MD 20742, USA
Received 18 August 1997; accepted 4 October 1998

abnormally folded and the properly folded product within the periplasm [4]. In addition, secretion of antibodies into the oxidizing environment of the periplasm can lead to antibody aggregation and precipitation [23]. Nonetheless, periplasmic secretion systems using various promoters have been used successfully for the expression of several Fab molecules and miniantibodies in *E. coli* [1,2,8,10,17]. These have given yields ranging from low milligram to gram levels of antibody per liter of media prior to purification.

High levels of heterologous protein expression in bacteria are often complicated by factors such as inclusion body formation, cellular toxicity due to the accumulation of foreign proteins and the degradation of desired product. Degradation of heterologous proteins by intracellular proteases has been observed in several expression systems [5,6,9,11,14]. The stringent stress response and the heat shock response, two defense-related cellular responses, are known to induce proteases in *E. coli* [15]. Stringent stress responses are triggered due to nutrient deficiency. Heat shock responses are triggered due to elevations in temperature, although heat shock proteins also appear during the stringent response. Overexpression of heterologous proteins can elicit product-degrading proteases [5], and lower temperatures and the avoidance of stress responses can give rise to higher heterologous protein yields [4,21]. This has been attributed, in part, to a reduced protein production rate which prevents the saturation of the transmembrane and folding processes, and thereby reduces the formation of partial and misfolded proteins which are open for proteolytic attack.

We present the screening and selection of a recombinant *E. coli* expression clone from the set of pHist clones generated above, the rapid development and scale-up of an *E. coli* anti-botulinum bt-Fab production process that employs a one-step IMAC purification process, and the control of fermentation conditions to minimize product degradation. Specifically, post-induction temperature and inducer concentration were varied to examine the effects of bt-Fab production rate on the yield of bt-Fab. Additionally, the relative activity of a protease increased significantly upon overexpression. Previous reports on this protease have demonstrated its upregulation upon overexpression of chloramphenicol acetyltransferase and during the stringent stress response [7,21]. In this work, this protease was found in the membrane fraction and was subsequently purified and shown to degrade the bt-Fab in incubation experiments. Moreover, an inverse correlation between the protease and bt-Fab was revealed *during* the fermentation through the construction of a simple mathematical model.

Materials and methods

Strains, plasmids, and clone evaluation

LB^{carb} plates of *E. coli* XL-1 blue host cells (Stratagene, La Jolla, CA, USA) containing bt-Fab candidate vectors were provided by Dr P Emanuel [3]. Inocula were prepared from single colonies in 250-ml starter flasks containing 50 ml of 1% glucose/LB^{carb}/pH 7.2. The shakers were maintained at 300 rpm and 37°C. Baffled 4-liter flasks containing 1 L of phosphate-buffered LB^{carb}, pH 7.2, 50 μg carb ml^{-1}, were inoculated with the 50-ml starting culture, grown at 25°C until the absorbance at 600 nm wavelength (A_{600}) reached 1.0, induced with 1 mM IPTG (*lac* promoter control) and then grown at 25°C for 60 h. Cells were harvested by centrifugation, resuspended in 50 mM sodium phosphate buffer (pH 7.8) containing 2 mM serine protease inhibitor, phenylmethylsulfonyl fluoride (PMSF), cracked by sonication, and the debris-free cell supernatant was obtained by centrifugation ($3000 \times g$). Cell supernatants were analyzed for the presence of bt-Fab by SDS-PAGE and Western blotting as described below. Cell supernatants of clones testing positive for bt-Fab were purified by IMAC chromatography and the concentration of the purified bt-Fab was determined as described below.

Fermentation conditions—induction temperature study

Inocula were prepared from glycerol stocks in 1-L baffled flasks containing 500 ml of 1% glucose/LB^{carb}/pH 7.2 at 37°C and 300 rpm until the A_{600} reached 3.0. The 14-L Microferm fermentors (New Brunswick Scientific, Edison, NJ, USA) containing 10 L of phosphate-buffered LB^{carb}, pH 7.2 were inoculated with the 500-ml starting cultures and maintained at 37°C until the A_{600} reached 1.0. At this point, the cells were induced with 1 mM IPTG and the temperature was immediately shifted to a test temperature. Three temperatures were evaluated: 25, 30 and 37°C. The dissolved oxygen level was maintained above 30% and the A_{600} was monitored throughout the fermentation. Cells were grown for 60 h after induction and two 30-ml samples were removed approximately every 5 h for analysis. The samples were centrifuged and the cell pellets were obtained.

Purification

A Bio-Cad chromatography controller (Perseptive Biosystems, Framingham, MA, USA) was used for the protein purification. The pH of the crude cell supernatant was adjusted to 7.8 and the sample was centrifuged at $10\,000 \times g$ for 30 min to remove particulates. This material was loaded onto a Ni^{2+}-NTA Sepharose metal-affinity chromatography column (Invitrogen Corporation, San Diego, CA, USA) pre-equilibrated in phosphate-buffered saline (PBS, 50 mM Na_2HPO_4/500 mM NaCl, pH 7.8) and washed with PBS until the absorbance at 280 nm wavelength (A_{280}) reached a stable baseline value of approximately 0.05. The column was further washed with five column volumes of 5 mM imidazole in PBS pH 7.8. Bound bt-Fab was eluted from the column with 150 mM imidazole in PBS pH 7.8 as shown in the Results. Column elution fractions were analyzed by total protein determination, SDS-PAGE and Western blotting.

Analytical

Sample preparation: Cell pellets were resuspended in PBS, at a ratio of 3 ml buffer per gram wet cell weight. Sample sets for Western analysis were mixed with the protease inhibitor, PMSF, to give a 2-mM PMSF final concentration. Sample sets for gelatin PAGEs (used for protease detection) had no protease inhibitors. Cells were cracked

by sonication (3 min, pulsed, Branson), centrifuged at 10 000 × *g* for 20 min and the debris-free cell supernatants were obtained.

Protein determination: Protein concentration was determined by a bicinchoninic (BCA) protein assay (Pierce, Rockford, IL, USA) with bovine serum albumin as the standard [22].

Western analysis: Samples containing 50 μg of total protein in non-reducing Laemmli buffer [12] were loaded onto polyacrylamide gels (12% separating gel, 4% stacking gel) and electrophoresed for ~1 h at 200 volts (Mini-PROTEAN II Electrophoresis Cells, Bio-Rad, Hercules, CA, USA). After electrophoresis, the gels were blotted onto nitrocellulose using a semi-dry transfer blotting apparatus (Bio-Rad). The nitrocellulose blots were blocked overnight at 4°C with 1% non-fat dry milk in PBS and washed with 0.1% Tween-20 in PBS. The blots were then incubated for 1 h at room temperature with an affinity isolated, alkaline phosphatase conjugated, pre-adsorbed goat antibody specific to the Fab segment of mouse IgG (Sigma Chemical Co, St Louis, MO, USA). The blots were washed and the signal was developed using BCIP/NBT (5-bromo-4-chloro-3-indolyl phosphate/nitro blue tetrazolium) color development reagent (Sigma). Blots were quantified by scanning densitometry (Stratagene Eagle-Eye II, NIH Image). Interestingly, in the absence of PMSF in extracts, no bt-Fab was detected.

SDS-GPAGE: Gels containing 6 mg of gelatin (hence GPAGE) were prepared as described previously [7]. The cellular supernatants in PBS (without further modification) were electrophoresed at 150 volts. After removal of SDS by washing with Triton X-100 for 1 h, the gels were incubated in 100 mM glycine, 2 mM ATP, 2 mM $MgCl_2$, pH 7.5 (incubation buffer) for 24 h at 37°C in order to restore enzymatic activity. Following regeneration, the gels were stained with amido black and destained [7]. Proteolytic activities, separated by molecular weight, were visualized by clear bands. The intensity of these bands is proportional to the mass, quantity and activity of the proteases present [7]. When extracts contained PMSF (as noted in samples for Western analysis), no activities were revealed.

Protease purification: The principal protease was subsquently purified using additional extractions steps (Gill RT, MS Thesis, University of Maryland, 1998) and preparative isoelectric focusing using a Rotofor (Bio-Rad), according to the manufacturer's directions. A 'strong extract' fraction containing only this protease was evaluated for bt-Fab activity. This was prepared following the general method utilized by Pacaud [16]. The crude cell lysate was spun at 40 000 × *g* for 1 h. The membrane pellet was resuspended in buffer B (50 mM Tris (pH = 7.5), 0.1% Triton X-100, 15% glycerol) to an approximate protein concentration of 2 mg ml^{-1}. This fraction was recentrifuged at 40 000 × *g* for 1 h. The supernatant was discarded and the pellet was resuspended in a minimal amount of buffer B. This fraction was again centrifuged at 40 000 × *g* for 1 h and resuspended in a mild extraction buffer C (buffer B + 500 mM NaCl), sonicated for 2 min, and mixed for 1 h. The suspension was centrifuged at 150 000 × *g* for 1 h. The supernatant was saved and labeled 'weak' fraction for later assay, the pellet was resuspended in a strong extraction buffer D, buffer A + 3% Emulphogen BC270, sonicated for 2 min, and mixed for 1 h. The suspension was centrifuged at 40 000 × *g* for 1 h. The supernatant was saved and labeled 'strong extract'. The pellet was discarded.

Results and discussion

Clone evaluation

The production of a recombinant immunoglobulin library in *E. coli* enabled the selection of a clone expressing bt-Fab with a high specificity towards the botulinum toxin [3]. The molecular weight of intact bt-Fab is approximately 50 kDa while that of the reduced form is approximately 24 kDa. Twenty-six recombinant pHist clones (from Emanuel) were grown and the bt-Fab purified as described above. Of these, 14 clones expressed the bt-Fab antibody fragment upon 1 mM IPTG induction when analyzed by Western blotting. The resultant bt-Fab of each clone was one-step purified by IMAC and screened for binding affinity. Table 1 lists the cellular yields and the purified bt-Fab yields of the 14 positive clones. The amount of purified bt-Fab obtained from these clones was typically 1 mg per liter of fermentation medium. The specific yields ranged from 70 to 367 μg of pure bt-Fab per g wet cells and were typically over 150 μg pure bt-Fab g^{-1} wet cells. The equilibrium dissociation constants of purified bt-Fab obtained from these clones ranged from 1.0×10^{-9} to 8.5×10^{-10} M min^{-1} and were comparable to that of anti- botulinum complex immunoglobulins which were around 7.0×10^{-9} M min^{-1} [3]. Clone pHist 5 was one of the lower yielding clones tested, however, it was selected for subsequent studies based on its affinity towards the toxin (1.0×10^{-9} M

Table 1 Results of screening of bt-Fab clones

pHist clone No.	Cell yield g L^{-1} media	Purified bt-Fab yield μg L^{-1} media	Specific yield μg pure bt-Fab g^{-1} cells
1B	8.2	1676	204
3	3.4	500	147
5	9.5	663	70
7	8.2	1580	193
9	7.8	1068	137
12	6.0	648	108
14	9.0	1112	124
16	5.7	568	100
17	7.8	1496	192
18	6.0	1564	261
19	5.0	1248	250
20	3.5	1283	367
26	3.5	477	136
143	5.5	1400	255

Baffled 4-L flasks containing 1 L of phosphate-buffered LB^{carb}, pH 7.2, 50 μg carb ml^{-1}, were grown at 25°C until A_{600} 1.0, then induced (1 mM IPTG) and maintained at 25°C for 60 h. Cells were centrifuged, resuspended, cracked and debris-free supernatant analyzed for bt-Fab, which was subsequently 1-step purified by IMAC. Wet cell weights are reported.

min^{-1}). Hence, efforts to increase fermentation yield were needed.

Cellular yield

The temperature variation experiments with pHist5 indicated that final cell yields were nearly identical at all three post-induction test temperatures and were near 4.5 g wet cells per liter of fermentation medium. Cell growth measurements as determined by the absorbance at 600 nm (A_{600}) over the course of the fermentations showed that growth at 25 and 30°C was very similar, both showing a slight decrease in A_{600} at the stationary phase (Figure 1). At 37°C, the culture showed a severe transient lag immediately after induction, but ultimately reached a stationary value comparable to that of the lower two temperatures. This dynamic lag occurred in several repeated experiments at 37°C. No death phase (decrease in A_{600}) was observed at 37°C.

Specified (bt-Fab) yield

The plasmid vector used in our studies contained the *pelB* leader sequence for translocating the bt-Fab to the *E. coli* periplasmic space in order to ensure proper folding and disulfide bond formation. However, translocation to the periplasm is often associated with the blockage of nascent protein at the inner membrane as well as proteolytic degradation of both the abnormally folded and the properly folded product within the periplasm [4,18]. Three successively lower post-induction temperatures (37, 30 and 25°C) were tested in order to decrease the expression rate and thereby avoid loss. Figure 2 illustrates the profile of bt-Fab during the post-induction period for the lower two temperatures; bt-Fab was not detected at 37°C. Figure 2a gives the normalized 50-kDa bt-Fab signal quantified from Western blots by scanning densitometry; the Western blots are shown in Figure 2b. At 30°C post-induction temperature, bt-Fab production reached a maximum relatively quickly around 9 h post-induction, and dropped rapidly to 10% of the maximum value by 33 h. In addition to the 50-kDa bt-Fab, Western analysis also showed the presence of lower molecular weight forms around 45 and 25 kDa which also

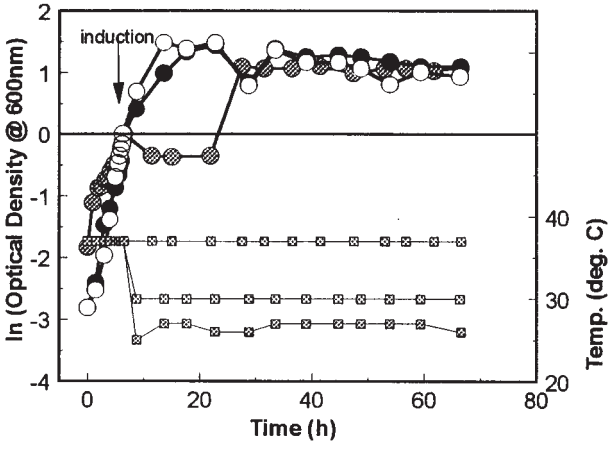

Figure 1 Effect of post-induction temperature on the growth of clone pHist 5. The studies were conducted in 14-L bioreactors as described in Materials and Methods. Cellular growth was determined by the absorbance at 600 nm (A_{600}). (●) 25°C, (○) 30°C, (▨) 37°C.

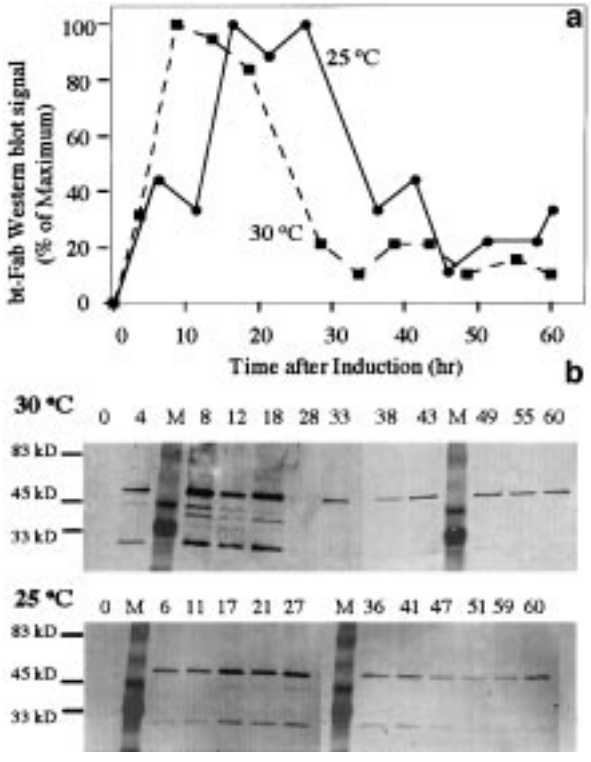

Figure 2 bt-Fab quantity in fermentations at 25 and 30°C. (a) Time course analysis of bt-Fab obtained from scanning densitometric analyses of Western blots. The *y*-axis represents the 50-kDa bt-Fab signal, the data for a given temperature is normalized with respect to the maximum 50-kDa signal obtained at that temperature. The maximum corresponds to *ca* 5 mg L^{-1} bt-Fab. (●) 25°C, (■) 30°C. There was only minimal bt-Fab detected at 37°C. (b) Western blots of bt-Fab in 30 and 25°C fermentations. Signals represent the amount of bt-Fab present in crude cell lysates containing 40 μg of total protein. M indicates molecular weight markers. Post-induction time increases from left (lane 1: 0 h) to right (lane 13: 60 h) as indicated. The appearance of degradation products at lower molecular weight was prevalent between 10 and 20 h post-induction.

increased in time and then eventually disappeared. At 25°C, the rate of bt-Fab production was slower compared to 30°C, reaching a maximum approximately 15 h after induction. Again, a decrease to 20% of the maximum value occurred after 25 h. Smaller quantities of lower molecular weight forms were seen at 25°C compared to 30°C, and they appeared and disappeared in a similar manner to the bt-Fab. In contrast to these two temperatures, there was no bt-Fab detected at 37°C. We suspected the perturbation in cell growth may have contributed to the loss of bt-Fab at 37°C. Subsequent investigations of intracellular protease activity were performed in cultures at all temperatures. Overall, the decrease in bt-Fab production with increasing post-induction temperature, and the appearance and subsequent disappearance of the lower molecular weight forms, suggested that proteolytic activity was responsible for bt-Fab loss.

Proteolytic activity

In order to examine the influence of proteolytic activity in this process, time-course samples of the same fermentations were analyzed by GPAGE as described in Materials and

Methods. The most predominant proteases are differentiated by both molecular weight and activity and are visualized as clear zones upon staining with amido black [7]. The intensities of these clear zones are proportional to the mass quantity and activity of the proteases present. Figure 3 shows the SDS-GPAGE results and their quantification by scanning densitometry. At all three temperatures, the predominant proteolytic activity was detected at 39 kDa. Moreover, a rapid increase in proteolytic activity, followed by a decrease, then another increase and ultimately a final decline was observed with increased induction time for 25°C and 37°C. Since there was negligible bt-Fab detected at 37°C and bt-Fab fragments in Western blots at the lower temperatures, we suspected a relationship between this protease activity and the loss of bt-Fab in the *E. coli* periplasm.

E. coli has at least 24 identified intracellular proteases, of which 12 are associated with the membrane while the others are present in the cytoplasm [13,14]. Interestingly, none of these proteases are reported to have a molecular weight of 39 kDa [7,21]. The closest is Omp T (also known as protease VII) which is a 34-kDa membrane-bound protein. In Figure 4, we demonstrate that the 39-kDa protease activity detected on the SDS-GPAGE gels originates in a membrane fraction. By protease inhibitor screening and SDS-GPAGE analyses, we have shown elsewhere that the 39-kDa protease has serine protease activity, similar to that of OmpT [20]. Additionally, as noted in Methods, PMSF inhibited this protease activity in extracts and also stabilized the bt-Fab. In the absence of PMSF, there was no bt-Fab detected in our Western blots at any fermentation temperature. In other work, we demonstrated that this activity was associated with the stringent stress response and heat shock response (consistent with OmpT), and is amplified upon overexpression of another heterologous protein, chloramphenicol acetyltransferase [7,20,21]. In Figure 4, we show that the 39-kDa protease, which was purified 290-fold (Gill RT, MS Thesis), degraded bt-Fab. Specifically, a strong extract fraction (Figure 4a), which contained only one protease band on an SDS-GPAGE, was incubated with the bt-Fab overnight (Figure 4b). In the absence of protease, the bt-Fab was stable, whereas increased protease in the incubation mixture accelerated the loss of bt-Fab on the Western blot.

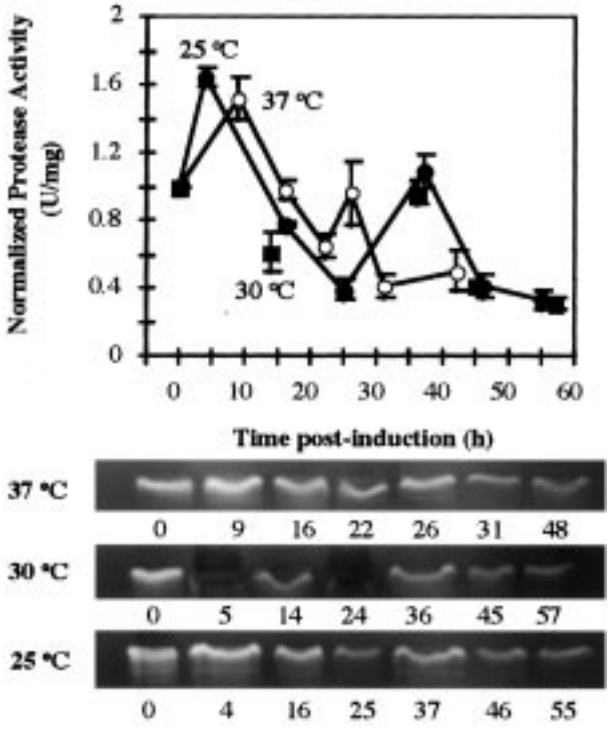

Figure 3 Analysis of intracellular protease activity. (a) Time course analysis of protease activity. Crude cell lysates were analyzed by SDS-GPAGE and quantified by scanning densitometry. The *y*-axis on the chart represents the 39-kDa protease activity normalized with respect to that of the pre-induction sample at each temperature. (b) GPAGE zymograms of the fermentation extracts quantified in upper panel. The only significant band on the SDS-GPAGEs was near 39 kDa. (●) 25°C, (■) 30°C, (○) 37°C.

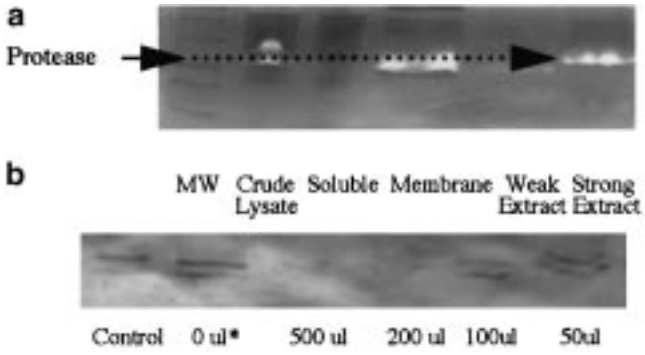

Figure 4 Digestion of bt-Fab by 39 kDa protease. (a) Characterization of the purification of 39 kDa protease by GPAGE analysis: lanes indicate crude lysate, soluble fraction, membrane fraction, weak extract of membrane fraction and strong extract of membrane fraction. SDS-GPAGE of strong membrane extracts revealed only one significant protease band at ~39 kDa. By SDS-PAGE this extract was purified 17-fold, subsequent preparative isoelectric focusing resulted in 290-fold purification and a single band on SDS-PAGE. (b) Western blot analysis of bt-Fab, in extracts of induced *E. coli*, incubated with various amounts of purified 39 kDa protease present in 'strong extracts', as indicated. The 'Control' lane contains purified bt-Fab.

A simple mathematical model was proposed to characterize the temporal regulation of the protease activities and to evaluate whether its coincident appearance was consistent with the degradation of bt-Fab shown in Western blots (Figure 4). The model presumes a second order rate law for bt-Fab degradation based on the coupled interaction of the antibody and protease. The details of the model are presented in the Appendix. In Figure 5, the model results are depicted. The cell density, protease activity, and bt-Fab quantity are shown as a function of time and are in excellent agreement with the data. That is, one would typically expect the bt-Fab to appear first and then disappear later when the protease activity increased, however our data show that both appeared at roughly the same time. The model demonstrates that the data can be explained by an interaction between the proteolytic activity and the bt-Fab appearing simultaneously, presumably because the bt-Fab synthesis overwhelms the increased protease activity. In this way, the model results corroborate our *in vitro* results showing that the disappearance of the bt-Fab during the post-induction period was related to the 39-kDa protease activity.

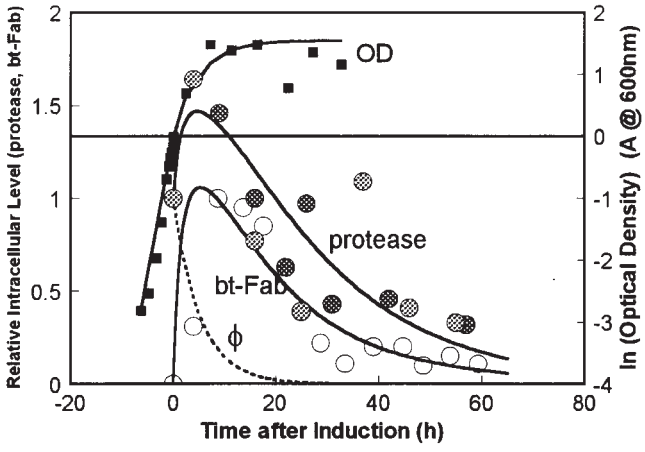

Figure 5 Model simulation of 30°C fermentation. Simulations indicate coincident timing of protease appearance and disappearance of bt-Fab. Data simulated include: optical density (■), normalized bt-Fab content (○), and normalized protease activity (⊗, 30 and 25°C; ●, 37°C). Also included is ϕ, the relative level of metabolic activity, or instantaneous growth rate of the culture (dotted line).

Purification

The affinity of amino acids such as histidines toward transition metals has resulted in the development of metal affinity separation techniques [19]. The 50-kDa bt-Fab molecule expressed in this study has six histidines attached at the C-terminus and, therefore, has high affinity to transition metals. Crude cellular extracts from a 10-L fermentation were centrifuged and the supernatants were loaded on to a Ni-NTA metal-affinity column. The bound protein was eluted using an imidazole elution gradient. Figure 6a shows a typical chromatography profile while Figure 6b shows the SDS-PAGE and Western analyses of the resulting protein fractions. Pure bt-Fab was visualized by a single band at around 50 kDa. The attachment of six histidine residues enabled a one-step purification process that resulted in a highly pure (>99%) product.

Processing considerations

Fermentation conditions such as higher post-induction temperatures, longer growth times, higher IPTG concentrations and enriched media adversely affected the subsequent purification process (only temperature results are shown here). Figure 7 shows a typical chromatography profile of a crude cell lysate obtained under adverse growth conditions (ie 37°C post-induction temperature). A large amount of bt-Fab either failed to bind to the column or was eluted during the PBS wash as shown by the first peak in the figure. The second peak was obtained during the 150-mM imidazole step and contained pure 50-kDa bt-Fab with high affinity to the metal affinity resin. The material that either failed to bind the column or was weakly bound contained high levels of lower molecular weight forms of bt-Fab as well as some 50-kDa bt-Fab (Western blot data not shown).

The failure of the early-eluting 50-kDa bt-Fab to bind the metal affinity resin indicates that the histidine tag was either made inaccessible due to improper protein folding or was fully or partially destroyed. Adverse growth conditions

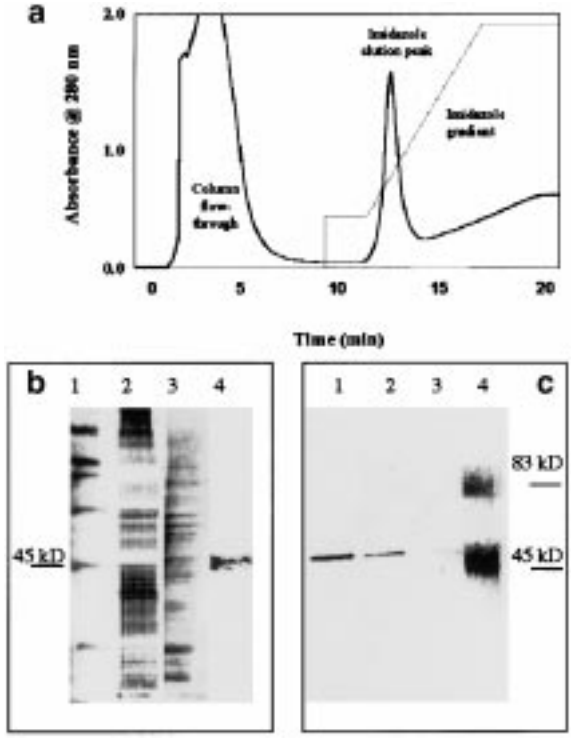

Figure 6 Purification of bt-Fab. (a) Chromatography profile of bt-Fab purification. (b) SDS-PAGE and (c) Western blot analyses of chromatography fractions. SDS-PAGE: Left to right, lane 1: molecular weight markers, 2: crude cell lysate (starting material), 3: column flow through (unbound fraction), 4: 150 mM imidazole elution peak (shown in (a)). Western blot: Left to right, lane 1: 150 mM imidazole elution peak, 2: crude cell lysate (starting material), 3: column flow through, 4: molecular weight markers.

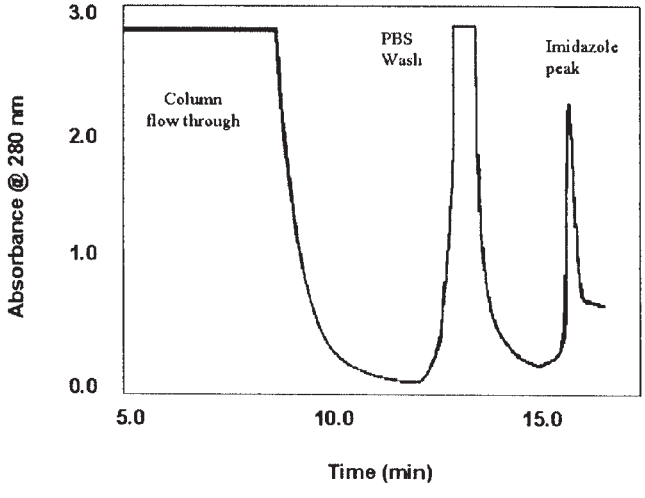

Figure 7 Typical chromatography profile of crude cell lysates obtained under adverse fermentation conditions (37°C post-induction temperature). Early peak (weakly bound and eluted by PBS wash) contained partially degraded bt-Fab in addition to intact Fab.

gave rise to crude extracts containing a high level of degraded and low metal-affinity 50-kDa bt-Fab which either failed to purify by metal-affinity chromatography or resulted in poor final bt-Fab yields. Conversely, the fermentation process described here (phosphate-buffered Lb^{carb}, 1 mM IPTG, 25°C post-induction temperature, etc) consistently resulted in IMAC purifiable bt-Fab. Our study demonstrated that the final outcome of the downstream process was strongly impacted by the upstream fermentation conditions.

In summary, this study has demonstrated that poly-histidine tagged recombinant antibody fragments with high immunospecificity can be successfully produced in *E. coli*. The incorporation of a poly-histidine tag at the heavy chain C-terminus enabled a single-step purification of the resultant antibody fragment. It was also shown that a 39-kDa protease activity (of similar size, activity, and proximity as OmpT) played an important role in the expression and stability of the heterologous bt-Fab molecule. Subsequent loss in cell extracts was attributed to the outer membrane protease. Lower post-induction temperatures, shorter growth times and lower IPTG concentration (not shown here) resulted in the formation of intact bt-Fab that could be efficiently purified by metal-affinity chromatography.

Acknowledgements

This research was funded principally by Grant No. DAAM01–96-C-0037 from the US Army Edgewood Research, Development and Engineering Center at Edgewood, Maryland. Partial support of this work was also provided by the National Science Foundation, Grant No. BES-9319366.

References

1 Better M, SL Bernhard, SP Lei, DM Fishwild, JA Lane, SF Carroll and AH Horwitz. 1993. Potent anti-CD5 ricin A chain immunoconjugates from bacterially produced Fab′ and F(ab′)2. Proc Natl Acad Sci USA 90: 457–461.
2 Carter P, RF Kelley, ML Rodrigues, B Snedecor, M Covarrubias, MD Velligan, WLT Wong, AM Rowland, CE Kotts, ME Carver, M Yang, JH Bourell, M Shepard and D Henner. 1992. High level *Escherichia coli* expression and production of a bivalent humanized antibody fragment. Bio/Technology 10: 163–167.
3 Emanuel P, T O'Brien, J Burans, BR DasGupta, JJ Valdes and M Eldefrawi. 1996. Directing antigen specificity towards botulinum neurotoxin with combinatorial phage display libraries. J Immunol Meth 193: 189–197.
4 Georgiou G, ML Shuler and DB Wilson. 1988. Release of periplasmic enzymes and other physiological effects of β-lactamase overproduction in *Escherichia coli* by manipulation of culture conditions. J Ferment Bioeng 69: 159–165.
5 Goff SA and AL Goldberg. 1985. Production of abnormal proteins in *E. coli* stimulates transcription of *lon* and other heat shock dependent genes. Cell 41: 587–595.
6 Gottesman S and M Maurizi. 1992. Regulation by proteolysis: energy-dependent proteases and their targets. Microbiol Rev 56: 592–621.
7 Harcum SW and WE Bentley. 1993. Response dynamics of 26, 34, 39, 54, and 80 kDa proteases in induced cultures of recombinant *Escherichia coli*. Biotechnol Bioengin 42: 675–685.
8 Horn U, W Strittmatter, A Krebber, U Knüpfer, M Kujau, R Wenderoth, K Müller, S Matzku, A Plückthun and D Riesenberg. 1996. High volumetric yields of functional dimeric miniantibodies in *Escherichia coli*, using an optimized expression vector and high-cell-density fermentation under non-limited growth conditions. Appl Microbiol Biotechnol 46: 524–532.
9 Kitano K, S Fugimoto, M Nakao, T Watanabe and Y Nakao. 1987. Intracellular degradation of proteins in relation to their location in *Escherichia coli* cells. J Biotechnol 5: 77–86.
10 Knappik A and A Plückthun. 1995. Engineered turns of a recombinant antibody improve its *in vivo* folding. Protein Eng 8: 81–89.
11 Kosinski M, U Rinas and J Bailey. 1992. Proteolytic response to the expression of an abnormal β-galactosidase in *Escherichia coli*. Appl Microbiol Biotechnol 37: 335–341.
12 Laemmli UK. 1970. Cleavage of structural proteins during the assembly of the head of bacteriophage. Nature 227: 680–685.
13 Lazdunski AM. 1989. Peptidases and proteases of *Escherichia coli* and *Salmonella typhimurium*. FEMS Microbiol Rev 63: 265–276.
14 Maurizi M. 1992. Protease and protein degradation in *Escherichia coli*. Experientia 48: 178–199.
15 Neidhardt F, R VanBogelan and V Vaughn. 1984. Genetics and regulation of heat shock proteins. Ann Rev Genet 18: 295–329.
16 Pacaud M. 1982. Purification and characterization of two novel proteolytic enzymes in membranes of *E. coli*. J Biol Chem 257: 4333–4339.
17 Pack P, M Kujau, V Schroeckh, U Knüpfer, R Wenderoth, D Riesenberg and A Plückthun. 1993. Improved bivalent miniantibodies, produced by high cell density fermentation of *Escherichia coli*. Bio/Technology 11: 1271–1277.
18 Plückthun A. 1991. Antibody engineering: advances from the use of *E. coli* expression systems. Bio/Technology 9: 545–551.
19 Porath J, J Carlsson, I Olsson and G Belfrage. 1975. Metal chelate affinity chromatography, a new approach to protein fractionation. Nature 258: 598–599.
20 Pulliam-Holoman T. 1996. PhD dissertation. University of Maryland, College Park.
21 Ramirez DM and WE Bentley. 1995. Fed-batch feeding and induction policies that improve foreign protein synthesis and stability by avoiding stress responses. Biotechnol Bioengin 47: 596–609.
22 Smith PK, RI Krohn, GT Hermanson, AK Mallia, FH Gartner, MD Provenzano, EK Fujimoto, NM Goeke, BJ Olson and DC Klenk. 1985. Measurement of proteins using bicinchoninic acid. Anal Biochem 150: 76–85.
23 Whitlow M and D Filpula. 1991. Single-chain F_V proteins and their fusion proteins. Methods. A companion to Meth Enzymol 2: 97–105.

Appendix

A mathematical model was developed to characterize the temporal and stoichiometric relationship between the appearance of a membrane-bound 39-kDa protease and the disappearance of the bt-Fab, which was translocated to the periplasmic space of the *E. coli*. The model includes equations for cell mass (OD, X), bt-Fab (bt), and protease activity (P):

$$\frac{dX}{dt} = \phi\mu_{max}X \tag{1}$$

$$\frac{d[bt]}{dt} = \phi k_{i,bt}X - k_d[P][bt] - k_{d,bt}[bt] - \mu[bt] \tag{2}$$

$$\frac{d[P]}{dt} = \phi k_{i,P}[P]X - k_{d,P}[P] - \mu[P] \tag{3}$$

$$\phi = e^{-k_\mu t} \tag{4}$$

The specific growth rate, μ, is calculated from the data using a least squares method and is represented as an exponential decay function, ϕ, multiplied by the maximum specific growth rate, μ_{max}, during the post-induction period (Eqns 1,4). This enables an empirically derived fit between the model simulation and the OD data (see Figure 4).

Table 2 Model constants

bt-Fab	$k_{bt,max}$	maximum bt-Fab synthesis rate	0.8	h^{-1}
	k_d	specific protease/bt-Fab degradation rate	0.03	h^{-1}
	$k_{d,bt}$	specific degradation rate	0.04	h^{-1}
Protease	$k_{P,max}$	maximum protease synthesis rate	0.7	h^{-1}
	$k_{d,P}$	specific protease degradation rate	0.045	h^{-1}
Cell mass	k_μ	metabolic decay time constant	0.19	h^{-1}

Model parameters were estimated based on: (1) initial synthesis rates; and (2) apparent rates of degradation after 30 h when there was no cell growth or product synthesis ($\mu = \phi = 0$). Data for constant determination were from the 30°C fermentation run, with the exception of the protease activity wherein the data of 25 and 30°C fermentations were grouped together enabling a more comprehensive dataset. There was no significant difference in protease profiles.

Further, we utilized ϕ as an attenuation factor for both bt-Fab and protease synthesis. That is, we have assumed that there was no synthesis of either bt-Fab or protease during the mid-to-late stationary phase (when $\phi = 0$). This assumption reflects the actual conditions, but more importantly maintains model simplicity. Thus, in Eqns 2 and 3, a maximum synthesis rate for each intracellular component (bt-Fab and protease) is multiplied by ϕ. In Eqn 2, the degradation of bt-Fab is described by a second order rate expression based on the coupled interaction of bt-Fab and protease. Both bt-Fab and protease also have an intrinsic degradation rate and a rate accounting for dilution due to biomass expansion ($-\mu$ term is needed for calculating intracellular quantities). Model parameters used for simulations are listed in Table 2. Simulations were performed using Euler's method.